THE JOURNAL OF PHYSICAL CHEMISTRY B

Article

pubs.acs.org/JPCB

Significantly Enhanced Adsorption of Bulk Self-Assembling Porphyrins at Solid/Liquid Interfaces through the Self-Assembly Process

Yonbon Arai* and Hiroshi Segawa*

Research Center for Advanced Science and Technology, The University of Tokyo, 4-6-1, Komaba, Meguro-ku, Tokyo

ABSTRACT: Controlling the adsorption behavior of bulk-phase self-assembling dye molecules at solid/liquid interfaces is of importance for application to various devices. Herein, we report an unexpected phenomenon on the adsorption behaviors of bulk J-aggregating water-soluble porphyrin diacids. A comparative study on the adsorption amounts of J-aggregated *meso*-tetrakis(4-sulfonatophenyl)-porphyrin diacid from freshly prepared and pre-aged solutions revealed enhanced adsorption through the self-assembly process (EASAP). The aggregate structure formed by EASAP is almost identical to the one from preformed J-aggregate solutions. The generation ratio of J-aggregates at an interface and in bulk strongly depends on the interface-to-volume ratio of the solutions. The surface property of cuvettes and coexisting inorganic ions has no significant effects on EASAP. While EASAP occurs in the J-aggregations of the other water-soluble porphyrin diacids, it is suggested that self-assembly properties play an important role in the adsorption proportion. These results will provide new insight into the adsorption equilibrium of bulk self-assembling molecules at solid/liquid interfaces.

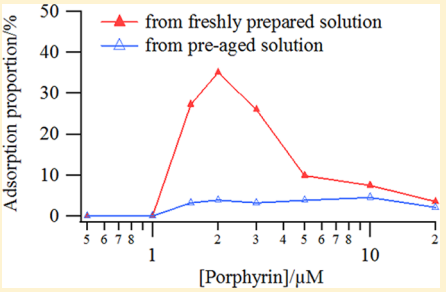

INTRODUCTION

The self-assembly of dye molecules by noncovalent interactions is a promising bottom-up approach for the fabrication of functional nanomaterials.[1−6] The deposition of resultant molecular assemblies onto solid surfaces is a prerequisite for application to various devices. Since numerous self-assembled architectures have been constructured in bulk solution, controlling the adsorption behavior of bulk self-assembling dye molecules at solid/liquid interfaces is of importance.

Self-assembled porphyrin architectures have attracted considerable interests due to functional versatility of the porphyrin unit as well as its relevance to molecular assemblies in the photosynthetic system.[4−6] In particular, the J-aggregate of a zwitterionic porphyrin, *meso*-tetrakis(4-sulfonatophenyl)-porphyrin diacid (H_4TSPP^{2-}, Figure 1)[7−11] has been intensively studied to date, since it shows various intriguing properties with regards to nanostructure,[12−17] electronic conductivity,[18−20] optical response,[21−24] supramolecular chirality,[25−33] and stimuli responsivity.[34−37] One of the major driving forces for the J-aggregate formation is electrostatic interactions between the negatively charged sulfonate groups and the positively charged porphyrin core.[38,39] It was proposed that the J-aggregation occurs in an autocatalytic pathway in which the formation of an aggregation nucleus is rate-determining.[40] Solution studies on the aggregate structure demonstrated the presence of a hollow cylinder with a one molecule-sized shell[41,42] in addition to larger structures with different morphologies.[13,43−46] Microscopic observations of J-aggregates deposited on substrates using AFM, STM, and TEM visualized rod- or tubelike nanostructures with well-defined dimensions,[12−17] where the nanorod morphology was presumed to originate from the flattening of the nanotube.[13,17] In the studies on the effect of stirring solution,[26,27,29,31] preferred deposition of J-aggregates in the conformation chosen in solution from the vortex chirality was reported to occur.[31] Although there are already a number of reports on deposited J-aggregates, a detailed study on their adsorption behavior at solid/liquid interfaces is still lacking. In this study, we found a significant effect of aging on the adsorption proportion of J-aggregated H_4TSPP^{2-}. The influence of self-assembly properties on the effect was also investigated by using other bulk-phase J-aggregating porphyrins, $H_4T(5\text{-}STh)P^{2-}$ and $H_4T(4\text{-}STh)P^{2-}$ (Figure 1).[47]

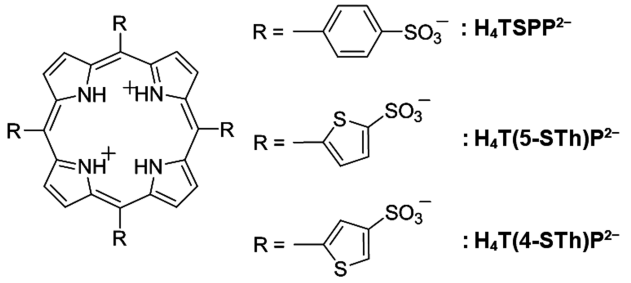

Figure 1. Porphyrin diacids used in this study.

Received: September 24, 2012
Published: October 11, 2012

   dx.doi.org/10.1021/jp309469j | *J. Phys. Chem. B* 2012, 116, 13575−13581

EXPERIMENTAL SECTION

Materials and Sample Preparation. H_4TSPP^{2-}, $H_4T(5\text{-}STh)P^{2-}$, and $H_4T(4\text{-}STh)P^{2-}$ were prepared by mixing a sufficient amount of protic acids into an aqueous solution of the sodium salts of the freebase forms (H_2TSPP^{4-}, $H_2T(5\text{-}STh)P^{4-}$, and $H_2T(4\text{-}STh)P^{4-}$, respectively). The sodium salt of H_4TSPP^{4-} was synthesized according to a reported literature.[48] Synthetic procedures of the sodium salts of $H_4T(5\text{-}STh)P^{4-}$ and $H_4T(4\text{-}STh)P^{4-}$ were described in our earlier paper.[49] Millipore water was used for all experiments.

Sample solutions of the porphyrin diacids were prepared by adding equivalent amounts of aqueous solutions of protic acids and/or salts into aqueous solutions of the freebase forms, followed by a rapid agitation. After mixing, the solutions were left to rest in the dark at room temperature for 4 h.

For AFM measurements, a glass cover was immersed in freshly prepared sample solutions and was left to rest for 4 h. After aging, the sample glass cover was briefly washed with a 0.5 M HCl solution. Prior to use, glass covers were cleansed by immersion in H_2O_2/H_2SO_4 (1:3) for 30 min, followed by rinsing in deionized water.

Measurements. To estimate adsorption amounts of porphyrin diacids at cuvettes, a 0.1 M NaOH aqueous solution was put into the cuvettes, wherein sample solutions were removed, and the concentrations of dissolved freebase porphyrins were determined spectrophotometrically. Since the complete removal of sample solutions from the cuvette wall was not easily accomplished, estimated adsorption amounts were a little overestimated. The proportions of porphyrin left inside the cuvettes were less than 5%.

UV−vis absorption measurements were performed using a V-570 UV−vis spectrophotometer (Jasco). AFM observations were performed using a SPM-9500 (Shimadzu) operating in noncontact mode in ambient conditions. Silicon cantilevers (Nanoworld) with a resonance frequency of ∼320 kHz were used.

RESULTS AND DISCUSSION

Adsorption Behavior of Self-Assembled H_4TSPP^{2-}. To obtain information on the aggregate adsorbed at the cuvette surface through the self-assembly process, freshly prepared solutions of H_4TSPP^{2-} with 0.5 M HCl were aged for 4 h in a 2 mm path length optical cell.[50] Figure 2 shows the UV−vis absorption spectra of the solution with the cell, the cell wherein the solution was removed, and the net solution. Remarkably, when a 2 μM porphyrin concentration is used (Figure 2a), the net absorption of the solution mainly consists of the monomer bands (λ_{max} = 435 and 645 nm), while the empty cell shows strong J-aggregate bands (λ_{max} = 491 and 707 nm), whose spectral feature is almost identical to that of the J-aggregate dispersed in bulk solution. In contrast, at 10 μM, the majority of J-aggregate absorption originates in the net solution (Figure 2b). The proportions of the adsorbed porphyrin to the total porphyrin amount (P_{ad}) at 2 and 10 μM were estimated as 71 ± 2 and 25 ± 2%, respectively. These results indicate that the proportion of J-aggregated H_4TSPP^{2-} adsorbed at the surface through the self-assembly process is strongly dependent on the porphyrin concentration.

To obtain more insight into the structure of the J-aggregates adsorbed during the self-assembly process, a glass substrate was immersed in freshly prepared solutions of H_4TSPP^{2-}, and the morphology of deposited aggregates was investigated by AFM.

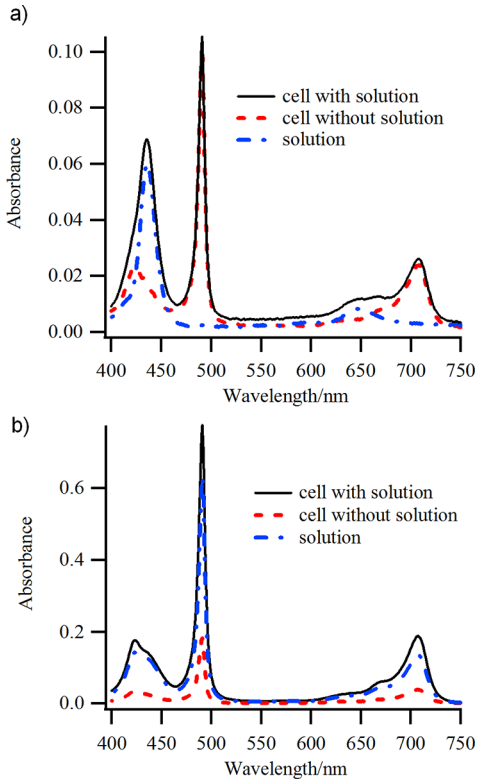

Figure 2. UV−vis absorption spectra of H_4TSPP^{2-} solutions prepared in an optical cell (solid line), the cell wherein the solution was removed (broken line), and the net solution (chain line). The solutions include (a) 2 and (b) 10 μM H_4TSPP^{2-} with 0.5 M HCl in water. The optical path length is 2 mm.

Figure 3 shows typical AFM images of deposited aggregates prepared from 2 and 10 μM H_4TSPP^{2-} solutions. Both the images mainly consist of rodlike nanostructures and their bundles. Individual nanorods have almost a constant height of ∼4 nm and a breadth of ∼40 nm in contrast to the length, which is broadly dispersed. Such a morphological feature is very similar to that of deposited J-aggregates prepared from solutions including preformed J-aggregates.[12,13,15−17] This indicates that the primary structure of the J-aggregate generated at the interfaces through the self-assembly process should be fundamentally identical to that of the J-aggregate formed in bulk solution. Thus, it is suggested that the observed nanorods consist of bimolecular layers formed by flattening of a tubelike nanostructure with a single-molecule shell.[13,17]

To obtain deeper insight into the adsorption behavior, the adsorption proportions of J-aggregated H_4TSPP^{2-} prepared by aging freshly prepared and 4 h pre-aged solutions in a glass tube cuvette were investigated. Figure 4 shows the plots of P_{ad} and the extinction coefficients at the monomer and J-aggregate band peaks (435 and 491 nm, respectively) as a function of concentration. Notably, the plot of P_{ad} from the freshly prepared solutions shows a sharp peak at around 2 μM, while the P_{ad} values from the pre-aged solutions[51] are almost constant and much smaller than the peak P_{ad} value. These results indicate that the significant adsorption occurs during the self-assembly process. Such an enhanced adsorption through the self-assembly process will be abbreviated to EASAP. It is noted that the P_{ad} value at 2 μM is obtained as ca. 38%, which is considerably different from the previously estimated value of 71 ± 2% using a 2 mm optical cell. The influence of the type of

dx.doi.org/10.1021/jp309469j | J. Phys. Chem. B 2012, 116, 13575−13581

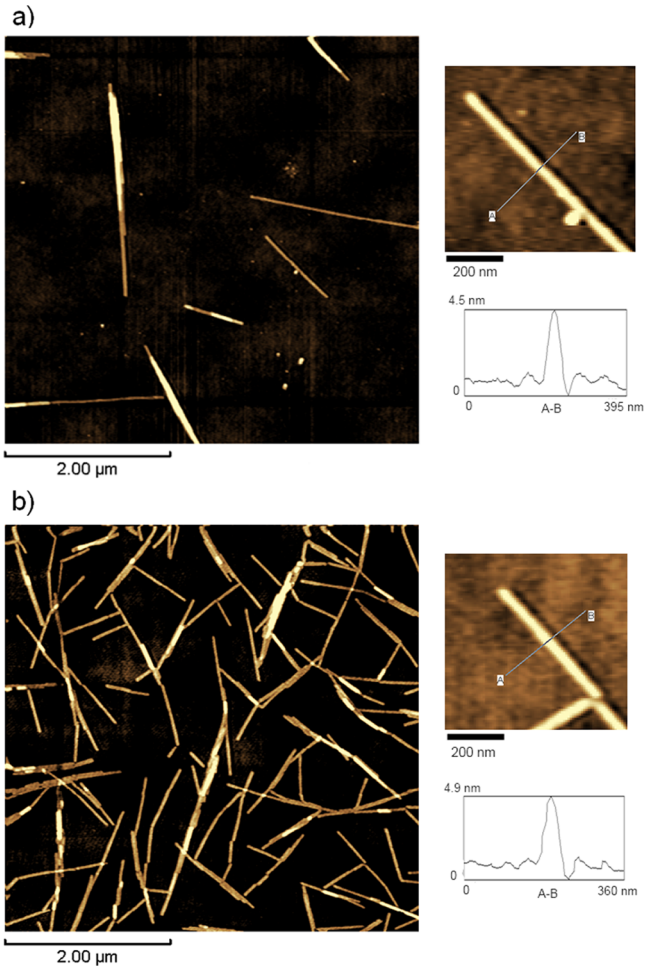

Figure 3. AFM images of H_4TSPP^{2-} J-aggregates adsorbed on a glass substrate from freshly prepared solutions with (a) 2 and (b) 10 μM H_4TSPP^{2-} with 0.5 M HCl.

cuvettes on the adsorption proportion will be discussed later. On the other hand, the concentration dependences of the extinction coefficients indicate that J-aggregates dispersed in bulk solution are generated less preferably than J-aggregates adsorbed at the solid/liquid interface, while the generation of bulk J-aggregates is dominant at higher concentrations. One origin of such a concentration dependency would be from the difference in the molecule-incorporating space of the interface and bulk. The larger molecule-incorporating space of the bulk should result in preferable generation of bulk J-aggregates under kinetic conditions, such as high concentrations.

On the basis of the plausible origin of the concentration dependence, the ratio of solid/liquid interface area to the solution volume should affect the generation ratio of the interface and bulk J-aggregates. To examine this, various thicknesses of rectangular quartz cuvettes were used for the same concentration of H_4TSPP^{2-} solutions. Figure 5 shows the plots of P_{ad} and extinction changes at the monomer and J-aggregate band peaks as a function of the solid/liquid interface area per 100 μL of solution. It is notable that the changes in P_{ad} and J-aggregate extinction are significantly large in contrast to the changes in the monomer extinction. These results indicate that the interface-to-volume ratio has a strong influence on the generation ratio of interface and bulk J-aggregates, while the aggregation equilibrium is less perturbed. The apparent

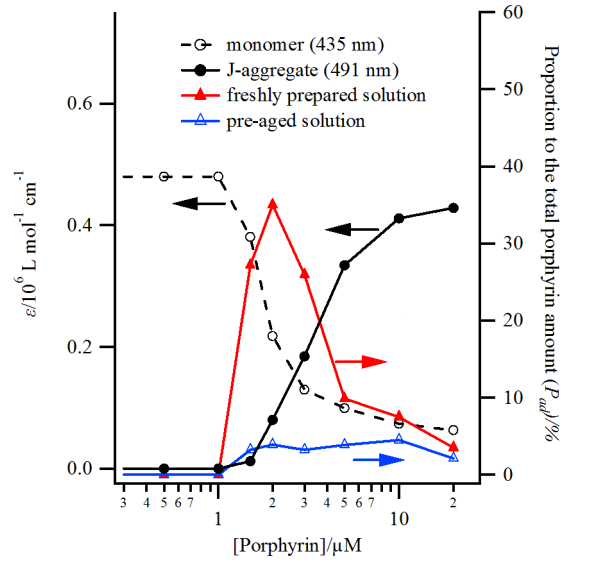

Figure 4. Concentration-dependent changes in extinction coefficients at the peak wavelengths of the monomer and J-aggregate bands of H_4TSPP^{2-} in water with 0.5 M HCl (left axis), and concentration-dependent changes in the proportions of H_4TSPP^{2-} adsorbed at the cuvette surface to the total porphyrin amount (P_{ad}, right axis). The solutions were prepared by aging freshly prepared and 4 h pre-aged solutions. For cuvettes, a glass tube was used.

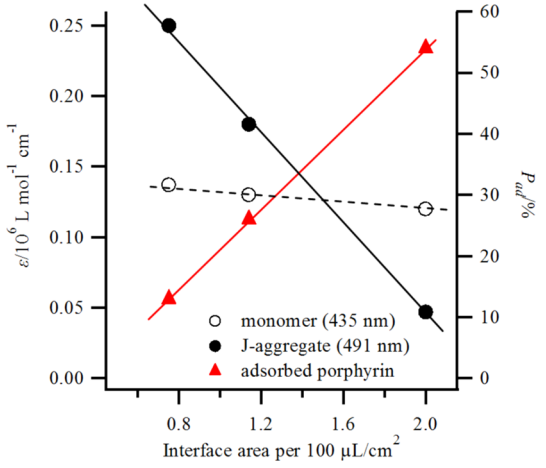

Figure 5. Extinction coefficients at the peak wavelengths of the monomer and J-aggregate bands of H_4TSPP^{2-} in water with 0.5 M HCl (left axis) and P_{ad} (right axis) as a function of the interface area per 100 μL of solution. The solutions were prepared by aging freshly prepared and 4 h pre-aged solutions. For cuvettes, rectangular quartz cells were used.

proportional relationships of the J-aggregate generations with the interface-to-volume ratio would originate in the dimensional difference between interface and bulk.

To make clear the influence of the surface property of cuvettes and coexisting inorganic ions on EASAP, adsorption proportions from freshly prepared and pre-aged solutions of 3 μM H_4TSPP^{2-} were investigated using various cuvettes and acids (with a salt). For cuvettes, quartz, glass, and polypropylene-based containers were used, and for the effect of inorganic ions, HCl, NaCl, and HNO_3 were used. Table 1 summarizes P_{ad} values obtained by various conditions. While the types of cuvettes and inorganic ions are influential on the P_{ad} values, all the P_{ad} values from the freshly prepared solutions

dx.doi.org/10.1021/jp309469j | J. Phys. Chem. B 2012, 116, 13575−13581

Table 1. P_{ad} Values Obtained by Aging Freshly Prepared and 4 h Pre-Aged Aqueous Solutions of 3 μM H_4TSPP^{2-}, Including Various Protic Acids (with a Salt) in Various Cuvettes

cuvette and acid (with salt)	P_{ad}/%	
	freshly prepared	pre-aged
rectangular quartz cell with 0.5 M HCl	30 ± 5	6 ± 5
glass tube with 0.5 M HCl	19 ± 3	6 ± 2
glass tube with 0.5 M HNO_3	26 ± 4	5 ± 2
glass tube with 0.05 M HCl and 0.5 M NaCl	21 ± 10	4 ± 2
polypropylene tube with 0.5 M HCl	39 ± 2	6 ± 1

are distinctly larger than those from the pre-aged solutions, indicating that these factors do not play a crucial role for EASAP.

To obtain deeper insight into the mechanism of EASAP, the time course of UV−vis spectral changes of the J-aggregate during the self-assembly process was investigated using a freshly prepared solution of 3 μM H_4TSPP^{2-} with a 10 mm path length optical cell. Interestingly, significant changes in the bandwidth of the J-aggregate (Soret band region) with time were found to be observed. Figure 6a shows absorption spectra of the J-aggregate band at various aging times, and Figure 6b shows the plots of its peak extinction coefficients and full width at half-maximum (FWHM) as a function of time. There is a tendency that FWHM increases following the increase in the extinction coefficient. While FWHM includes both the bands of the interface and bulk J-aggregates, the contribution of the interface J-aggregate would be much smaller at least after 20 min since the absorbance of the J-aggregate adsorbed at the cell wall was estimated to be less than 10% of the total absorbance after 120 min of aging. It is likely that the band broadening originates in the formation of hierarchical assemblies, which could cause changes in the electronic absorption or light scattering of J-aggregates. The formation of hierarchical assemblies was demonstrated by other techniques, such as light-scattering analyses[44−46] and microscopic observations.[13]

To compare FWHM's of the interface and bulk J-aggregates after 120 min of aging, 0.5 M HCl aqueous solution was added to the cell, wherein the solution was removed, and the UV−vis spectrum of the cell was measured, where the dissolution of adsorbed porphyrins into the bulk solution was negligible during the measurement. Figure 6c shows the absorption bands of the interface and bulk J-aggregates after 120 min of aging. Notably, compared with the bulk J-aggregate, the interface J-aggregate has a narrower bandwidth (FWHM is ~8.5 nm), which is comparable to the FWHM between 20 and 30 min. It is likely that the interface J-aggregate has a hierarchically less grown structure compared with the bulk one after 120 min of aging, while any contribution of the interactions between the aggregate and the solid surface on the bandwidth could not be excluded.

On the Mechanism of EASAP. The experimental results revealed that a significant proportion of H_4TSPP^{2-} molecules up to more than 70% can adsorb at solid/liquid interfaces by EASAP. The origins of such a strong adsorption proportion should be from cooperative noncovalent interactions, including intermolecular interactions and interactions between the J-aggregate and solid surface, since significant adsorption of monomeric H_4TSPP^{2-} was not observed (data are not shown) and there were no specific interactions of the J-aggregate with the solid surfaces, as discussed with Table 1. On the other hand,

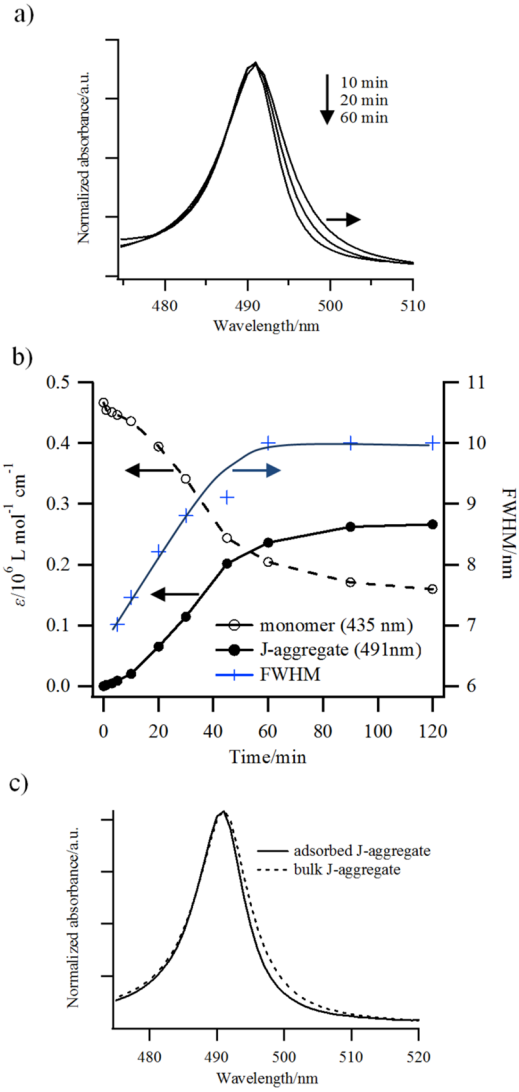

Figure 6. Time course of UV−vis spectra of a freshly prepared solution of 3 μM H_4TSPP^{2-} J-aggregates in water with 0.5 M HCl. For the cuvette, a 10 mm path length optical cell was used. (a) Band shapes of the J-aggregates (Soret) at various aging times. (b) Time courses of extinction coefficients at the peaks of the monomer and J-aggregate (left axis) and FWHM of the J-aggregate band (right axis). (c) Band shapes of the J-aggregates adsorbed at the cell wall (solid line) and dispersed in bulk solution (broken line) after 120 min of aging. The adsorbed J-aggregate was immersed in 0.5 M HCl.

the observation of a much smaller adsorption proportion by aging pre-aged solutions than from freshly prepared solutions indicates that the morphology of the J-aggregate plays an important role for the stability of the adsorption state. Here, the equilibrium constant (K_{ad}) of adsorption of a J-aggregate (J) at a solid/liquid interface (S) is described below.

$$J + S \rightleftharpoons J{-}S \quad K_{ad}$$

Two plausible mechanisms for EASAP could be made. One is that J-aggregates can be formed at the solid/liquid interfaces and resultant interface J-aggregates have larger K_{ad} values than J-aggregates formed in bulk solution. If this model holds true, it should be expected that the morphology and aggregation thresholds of interface J-aggregates are distinct from those of bulk J-aggregates due to the significant difference in the environments of the interface and bulk for nucleation and

dx.doi.org/10.1021/jp309469j | J. Phys. Chem. B 2012, 116, 13575−13581

growth. However, there appears to be only minor differences in morphology between the J-aggregates from freshly prepared and pre-aged solutions, as discussed with Figure 3. Also, as discussed with Figure 5, changes in the generation ratio of interface and bulk J-aggregates at the same concentrations do not have a significant influence on the monomer–aggregate equilibrium, indicating that the aggregation thresholds of interface and bulk J-aggregates are similar.

The other plausible mechanism is that J-aggregates formed in bulk solution at the earlier stages have larger K_{ad} values than hierarchically grown J-aggregates formed at the latter stages (Figure 7). This model is in good agreement with the

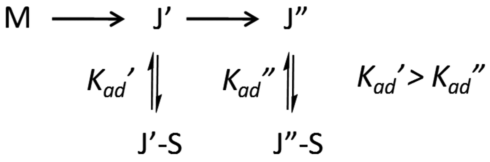

Figure 7. Schematic depicting a plausible mechanism of EASAP. M is the monomer, J′ is a J-aggregate formed in bulk solution at an early stage, and J″ is a hierarchically more grown J-aggregate at the later stage. In the course of the evolution, J′ and J″ can adsorb at a solid/liquid interface (S) by the equilibria of K_{ad}' and K_{ad}'', respectively. Under the condition of $K_{ad}' > K_{ad}''$, more adsorption of the molecules occurs through the self-assembly process (from a freshly prepared solution) than from a pre-aged solution.

experimental results shown in Figure 6 and does not contradict the similarity in the morphology and aggregation thresholds of interface and bulk J-aggregates. Thus, this mechanistic model for EASAP is more likely than the former one. The origin of the morphology dependency of K_{ad} could be from the ratio of the interface area of solvent/aggregate to the interface area of aggregate/solid surface, where larger ratios of the interface areas should lead to smaller K_{ad} values. Since the hierarchical assemblies would be porous structures considering the tubelike primary structure,[16,41,42] the interface area ratio of hierarchically grown J-aggregates would be larger than that of less grown ones.

Adsorption Behaviors of Self-Assembled $H_4T(5\text{-}STh)P^{2-}$ and $H_4T(4\text{-}STh)P^{2-}$. In our previous work,[47] we reported that $H_4T(5\text{-}STh)P^{2-}$ and $H_4T(4\text{-}STh)P^{2-}$ form J-aggregates in acidic aqueous solutions with increasing concentrations or ionic strength. While the aggregate structure and aggregation threshold of the $H_4T(5\text{-}STh)P^{2-}$ J-aggregate are analogous to those of the H_4TSPP^{2-} one, $H_4T(4\text{-}STh)P^{2-}$ J-aggregate has sheetlike nanostructures and a distinctively higher aggregation threshold than the other J-aggregates. To obtain insight into the influence of molecular structure and self-assembly properties on EASAP, the adsorption behaviors of $H_4T(5\text{-}STh)P^{2-}$ and $H_4T(4\text{-}STh)P^{2-}$ J-aggregates were examined. Figure 8 shows the concentration dependences of the adsorption proportions from freshly prepared and 4 h pre-aged solutions in addition to the extinction coefficients at the peaks of the monomer bands (458 and 452 nm for $H_4T(5\text{-}STh)P^{2-}$ and $H_4T(4\text{-}STh)P^{2-}$, respectively) and the J-aggregate bands (507 and 499 nm for $H_4T(5\text{-}STh)P^{2-}$ and $H_4T(4\text{-}STh)P^{2-}$, respectively). The plots demonstrate that the $H_4T(5\text{-}STh)P^{2-}$ aggregation sufficiently occurs at the relatively small concentration of <2 μM, similar to the H_4TSPP^{2-} one, whereas the $H_4T(4\text{-}STh)P^{2-}$ aggregation requires at least 100 μM. Though there is this considerable difference in their aggregation thresholds, both the J-aggregates,

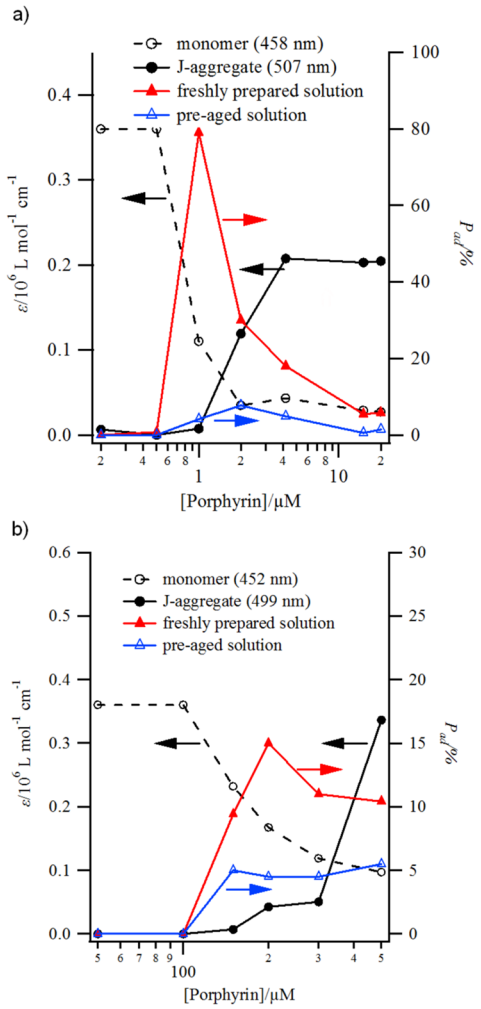

Figure 8. Concentration-dependent changes in extinction coefficients at the peak wavelengths of the monomer and J-aggregate bands of (a) $H_4T(5\text{-}STh)P^{2-}$ and (b) $H_4T(4\text{-}STh)P^{2-}$ in acidic water (left axis), and concentration-dependent changes in their P_{ad} from freshly prepared and 4 h pre-aged solutions (right axis). For $H_4T(5\text{-}STh)P^{2-}$, a glass tube was used with 0.5 M HCl, and, for $H_4T(4\text{-}STh)P^{2-}$, a plastic tube was used with 0.5 M HNO_3.[52,53]

similar to the H_4TSPP^{2-} one, show distinctly larger P_{ad} values by adsorption from the freshly prepared solutions than from the pre-aged ones at low concentrations. These results indicate that EASAP is a common phenomenon for the J-aggregates of water-soluble porphyrin diacids. It should be notable that the maximum adsorption proportions of $H_4T(5\text{-}STh)P^{2-}$ and $H_4T(4\text{-}STh)P^{2-}$ are substantially different.[52] To make such a difference more clear, the maximum P_{ad} values of $H_4T(5\text{-}STh)P^{2-}$ (1 μM) and $H_4T(4\text{-}STh)P^{2-}$ (200 μM) were investigated under the same interface-to-volume ratio of the solutions (~1.1 cm^2 per 100 μL) using a rectangular quartz cell. The obtained P_{ad} value of $H_4T(5\text{-}STh)P^{2-}$ was ~74%, which is comparable to that of H_4TSPP^{2-} (71 ± 2%), whereas $H_4T(4\text{-}STh)P^{2-}$ showed a distinctly smaller one of 9 ± 1%. Taking into consideration the similar molecular structure, the distinguished adsorption proportion should originate from a difference in their self-assembly properties. Their distinguished self-assembled structures[47] and the substantial difference in their aggregation thresholds could be the origin. To understand the detailed mechanism of the effect of self-assembly properties

dx.doi.org/10.1021/jp309469j | J. Phys. Chem. B 2012, 116, 13575–13581

on EASAP, a more elaborate systematic study using other self-assembling molecules would be necessary.

CONCLUSIONS

The adsorption proportion of bulk-phase self-assembling porphyrins at solid/liquid interfaces can be substantially enhanced through the self-assembly process compared with adsorption from well-aged solutions. Self-assembly properties can have a significant influence on the adsorption proportion by EASAP. Since the structure and aggregation threshold of interface J-aggregates generated by EASAP are almost identical to those formed by adsorption from pre-aged solutions, it is not likely that EASAP originates in surface-induced self-assembly, as observed in a bulk self-assembling dye system.[55] It is suggested that EASAP is caused by adsorption−desorption equilibrium shifts by the formation of hierarchical assemblies of J-aggregates in bulk solution. These results may provide deeper insight into the elusive J-aggregation[31] and will offer new knowledge for the adsorption behavior of self-assembled molecular nanomaterials at solid/liquid interfaces.

AUTHOR INFORMATION

Corresponding Author

*E-mail: arai@dsc.rcast.u-tokyo.ac.jp (Y.A.), csegawa@mail.ecc.u-tokyo.ac.jp (H.S.).

Notes

The authors declare no competing financial interest.

ACKNOWLEDGMENTS

We thank Prof. T. Kubo, Dr. K. Tamaki, and Dr. J. T. Dy for valuable discussions. This work was supported by the Funding Program for World-Leading Innovative R&D on Science and Technology (FIRST) "Development of Organic Photovoltaics toward a Low-Carbon Society" from the Cabinet Office of Japan.

REFERENCES

(1) Lehn, J. *Supramolecular Chemistry: Concepts and Perspectives*; VCH-Wiley: Weinheim, Germany, 1995.
(2) Hoeben, F. J. M.; Jonkheijm, P.; Meijer, E. W.; Schenning, A. P. H. J. *Chem. Rev.* **2005**, *105*, 1491−1546.
(3) Ariga, K.; Hill, J. P.; Lee, M. V.; Vinu, A.; Charvet, R.; Acharya, S. *Sci. Technol. Adv. Mater.* **2008**, *9*, 014109−014196.
(4) Drain, C. M.; Alessandro, V.; Radivojevic, I. *Chem. Rev.* **2009**, *109*, 1630−1658.
(5) Beletskaya, I.; Tyurin, V. S.; Tsivadze, A. Y.; Guilard, R.; Stern, C. *Chem. Rev.* **2009**, *109*, 1659−1713.
(6) Medforth, C. J.; Wang, Z.; Martin, K. E.; Song, Y.; Jacobsenc, J. L.; Shelnutt, J. A. *Chem. Commun.* **2009**, 7261−7277.
(7) Fleischer, E. B.; Palmer, J. M.; Srivastava, T. S.; Chatterjee, A. *J. Am. Chem. Soc.* **1971**, *93*, 3162−3167.
(8) Pasternak, R. F.; Huber, P. R.; Boyd, P.; Engasser, G.; Francesconi, L.; Gibbs, E.; Fasella, P.; Cerio Venturo, G.; Hinds, L.; de, C. *J. Am. Chem. Soc.* **1972**, *94*, 4511−4517.
(9) Ohno, O.; Kaizu, Y.; Kobayashi, H. *J. Chem. Phys.* **1993**, *99*, 4128−4139.
(10) Ribó, J. M.; Crusats, J.; Farrera, J. A.; Valero, M. L. *J. Chem. Soc., Chem. Commun.* **1994**, 681−682.
(11) Pasternack, R. F.; Schaefer, K. F.; Hambright, P. *Inorg. Chem.* **1994**, *33*, 2062−2065.
(12) Schwab, A. D.; Smith, D. E.; Rich, C. S.; Young, E. R.; Smith, W. F.; de Paula, J. C. *J. Phys. Chem. B* **2003**, *107*, 11339−11345.
(13) Rotomskis, R.; Augulis, R.; Snitka, V.; Valiokas, R.; Liedberg, B. *J. Phys. Chem. B* **2004**, *108*, 2833−2838.
(14) Snitka, V.; Rackaitis, M.; Rodaite, R. *Sens. Actuators, B* **2005**, *109*, 159−166.
(15) Friesen, B. A.; Nishida, K. R. A.; McHale, J. L.; Mazur, U. *J. Phys. Chem. C* **2009**, *113*, 1709−1718.
(16) Vlaming, S. M.; Augulis, R.; Stuart, M. C. A.; Knoester, J.; van Loosdrecht, P. H. M. *J. Phys. Chem. B* **2009**, *113*, 2273−2283.
(17) Friesen, B. A.; Rich, C. C.; Mazur, U.; McHale, J. L. *J. Phys. Chem. C* **2010**, *114*, 16357−16366.
(18) Schwab, A. D.; Smith, D. E.; Bond-Watts, B.; Johnston, D. E.; Hone, J.; Johnson, A. T.; de Paula, J. C.; Smith, W. F. *Nano Lett.* **2004**, *4*, 1261−1265.
(19) Riley, C. K.; Muller, E. A.; Feldman, B. E.; Cross, C. M.; Aken, K. L. V.; Johnston, D. E.; Lu, Y.; Johnson, A. T.; de Paula, J. C.; Smith, W. F. *J. Phys. Chem. C* **2010**, *114*, 19227−19233.
(20) Friesen, B. A.; Wiggins, B.; McHale, J. L.; Mazur, U.; Hipps, K. W. *J. Am. Chem. Soc.* **2010**, *132*, 8554−8556.
(21) Ogawa, T.; Tokunaga, E.; Kobayashi, T. *Chem. Phys. Lett.* **2005**, *408*, 186−191.
(22) Collini, E.; Ferrante, C; Bozio, R. *J. Phys. Chem. B* **2005**, *109*, 2−5.
(23) Collini, E.; Ferrante, C.; Bozio, R.; Lodi, A.; Ponterini, G. *J. Mater. Chem.* **2006**, *16*, 1573−1578.
(24) Nakata, K.; Kobayashi, T.; Tokunaga, E. *Phys. Chem. Chem. Phys.* **2011**, *13*, 17756−17767.
(25) Purrello, R.; Scolaro, L. M.; Bellacchio, E.; Gurrieri, S.; Romeo, A. *Inorg. Chem.* **1998**, *37*, 3647−3648.
(26) Ribó, J. M.; Crusats, J.; Sagues, F.; Claret, J.; Rubires, R. *Science* **2001**, *292*, 2063−2066.
(27) Rubires, R.; Farrera, J.; Ribó, J. M. *Chem.—Eur. J.* **2001**, *7*, 436−446.
(28) El-Hachemi, Z.; Escudero, C.; Arteaga, O.; Canillas, A.; Crusats, J.; Mancini, G.; Purrello, R.; Sorrenti, A.; D'Urso, A.; Ribó, J. M. *Chirality* **2009**, *21*, 408−412.
(29) Arteaga, O.; Canillas, A.; Purrello, R.; Ribó, J. M. *Opt. Lett.* **2009**, *34*, 2177−2179.
(30) Nagahara, T.; Kisoda, K.; Harima, H.; Aida, M.; Ishibashi, T.-a. *J. Phys. Chem. B* **2009**, *113*, 5098−5103.
(31) D'Urso, A.; Randazzo, R.; Taro, L. L.; Purrello, R. *Angew. Chem., Int. Ed.* **2010**, *49*, 108−112.
(32) Castriciano, M. A.; Romeo, A.; De Luca, G.; Villari, V.; Scolaro, L. M.; Micali, N. *J. Am. Chem. Soc.* **2011**, *133*, 765−767.
(33) Kitagawa, Y.; Segawa, H.; Ishii, K. *Angew. Chem., Int. Ed.* **2011**, *50*, 9133−9136.
(34) Fujii, Y.; Hasegawa, Y.; Yanagida, S.; Wada, Y. *Chem. Commun.* **2005**, 3065−3067.
(35) Luca, G. D.; Pollicino, G.; Romeo, A.; Scolaro, L. M. *Chem. Mater.* **2006**, *18*, 2005−2007.
(36) Egawa, Y.; Hayashida, R.; Anzai, J. *Langmuir* **2007**, *23*, 13146−13150.
(37) Liu, L.; Li, Y.; Liu, M. *J. Phys. Chem. C* **2008**, *112*, 4861−4866.
(38) Akins, D. L.; Zhu, H.-R.; Guo, C. *J. Phys. Chem.* **1994**, *98*, 3612−3618.
(39) Akins, D. L.; Zhu, H.-R.; Guo, C. *J. Phys. Chem.* **1996**, *100*, 5420−5425.
(40) Pasternack, R. F.; Fleming, C.; Herring, S.; Collings, P. J.; de Paula, J.; DeCastro, G.; Gibbs, E. J. *Biophys. J.* **2000**, *79*, 550−560.
(41) Gandini, S. C. M.; Gelamo, E. L.; Itri, R.; Tabak, M. *Biophys. J.* **2003**, *85*, 1259−1268.
(42) Kitahama, Y.; Kimura, Y.; Takazawa, K. *Langmuir* **2006**, *22*, 7600−7604.
(43) Collings, P. J.; Gibbs, E. J.; Starr, T. E.; Vafek, O.; Yee, C.; Pomerance, L. A.; Pasternack, R. F. *J. Phys. Chem. B* **1999**, *103*, 8474−8481.
(44) Micali, N.; Romeo, A.; Laucieri, R.; Purrello, R.; Mallamace, F.; Scolaro, L. M. *J. Phys. Chem. B* **2000**, *104*, 9416−9420.
(45) Micali, N.; Mallamace, F.; Romeo, A.; Purrello, R.; Scolaro, L. M. *J. Phys. Chem. B* **2000**, *104*, 5897−5904.
(46) Micali, N.; Villari, V.; Castriciano, M. A.; Romeo, A.; Scolaro, L. M. *J. Phys. Chem. B* **2006**, *110*, 8289−8295.

(47) Arai, Y.; Segawa, H. *Chem. Commun.* **2010**, *46*, 4279−4281.
(48) Srivastava, T. S.; Tsutsui, M. *J. Org. Chem.* **1973**, *38*, 2103.
(49) Arai, Y.; Nakazaki, J.; Segawa, H. *Tetrahedron Lett.* **2008**, *49*, 5810−5812.
(50) It was observed that spectral changes of the 2 μM solution reach a plateau after 4 h of aging.
(51) For the total porphyrin amount of pre-aged solutions, the amount of porphyrin adsorbed at the cuvette surface during the pre-aging process was subtracted.
(52) To avoid excessive usage of $H_4T(4\text{-STh})P^{2-}$, a plastic tube, which is smaller than the glass tube, was used. Similar to H_4TSPP^{2-}, the type of the cuvettes did not play a crucial role in EASAP of the aggregates of $H_4T(5\text{-STh})P^{2-}$ and $H_4T(4\text{-STh})P^{2-}$.
(53) Because of the Cl^- specific aggregation of $H_4T(4\text{-STh})P^{2-}$, HNO_3 was used as a protic acid for this porphyrin. See ref 54 for the detailed aggregation behavior of $H_4T(4\text{-STh})P^{2-}$.
(54) Arai, Y.; Tsuzuki, K.; Segawa, H. *Phys. Chem. Chem. Phys.* **2012**, *14*, 1270−1276.
(55) Yao, H.; Ikeda, H.; Kitamura, N. *J. Phys. Chem. B* **1998**, *102*, 7691−7694.